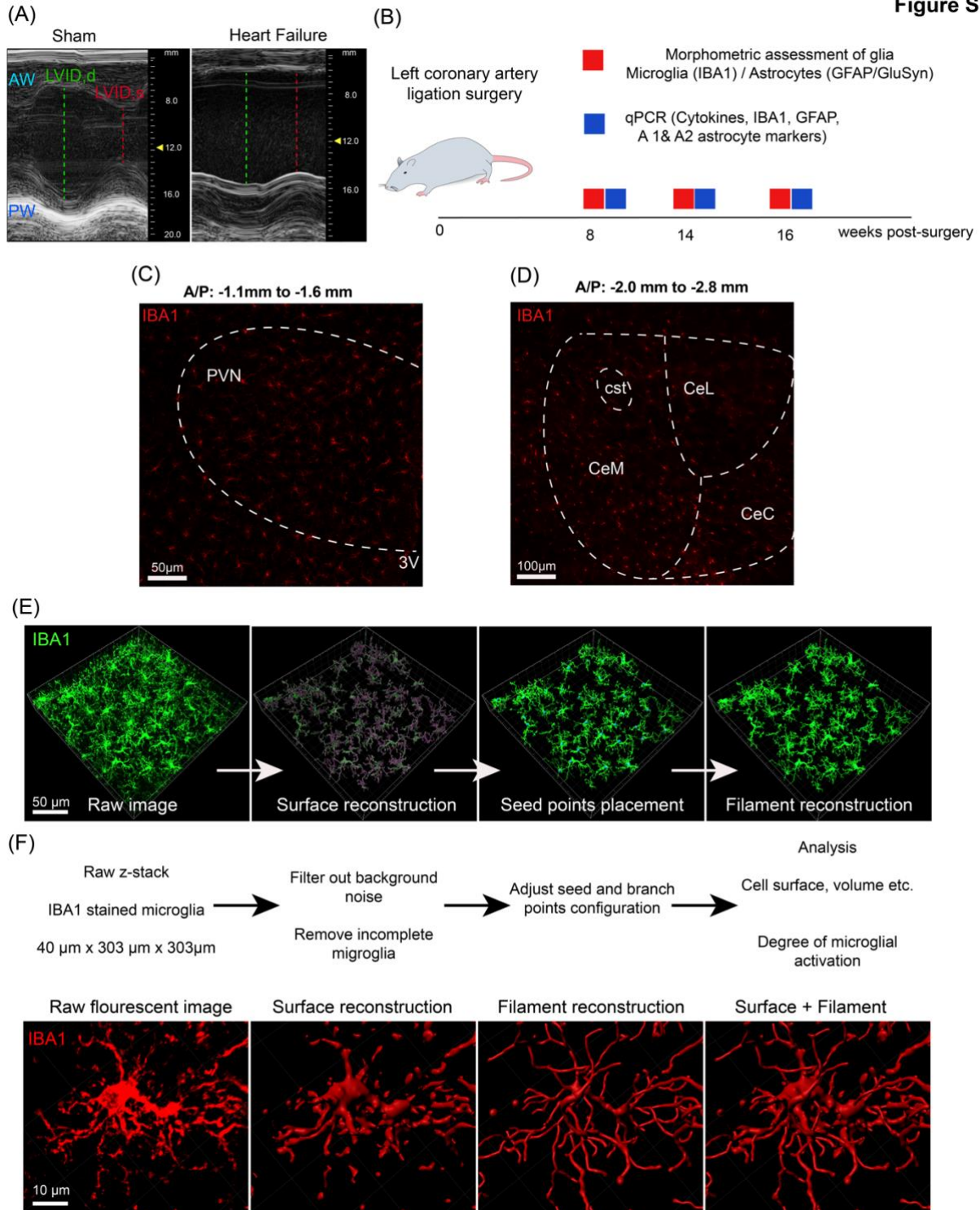


**Three-dimensional morphometric analysis reveals time-dependent structural changes in microglia and astrocytes in the central amygdala and hypothalamic paraventricular nucleus of heart failure rats**

Ferdinand Althammer, Hildebrando Candido Ferreira-Neto, Myurajan Rubaharan, Ranjan Kumer Roy, Atit A. Patel, Daniel N. Cox and Javier E. Stern

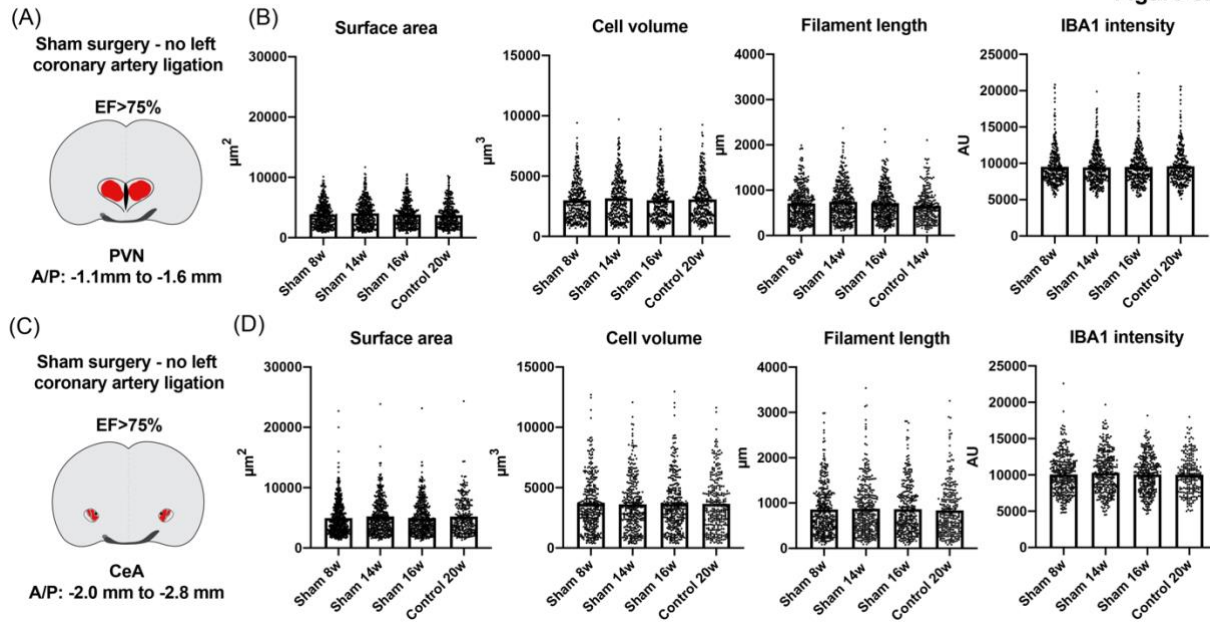
## **Supplementary Materials**

Figure S1



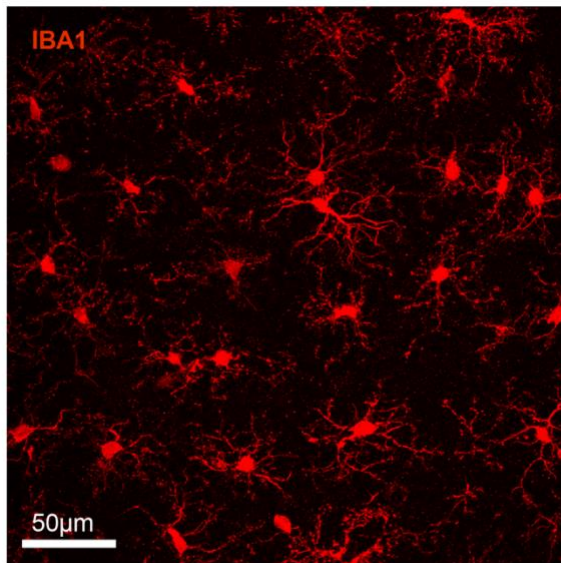
**Figure S1: Heart failure surgery, qPCR and three-dimensional reconstruction** (a) representative image showing the echocardiographic assessment left ventricular cardiac function in a sham and HF rats, (b) timetable depicting morphometric assessments and qPCR at 8-, 14- and 16- weeks post-surgery, (c, d) representative confocal images showing IBA1-labeled microglia (red) in the PVN and CeA and the topographic delineation of the nuclei, (e) schematic depiction of the sequential steps used for the 3D morphometric reconstruction and assessment of microglia (IBA1, green), (f) confocal images show the step-by-step process for three-dimensional reconstruction of a single microglia (IBA1, red). For image processing, colors were changed from red to green in IMARIS for better visibility and increased precision during manual editing of reconstructed microglia. Note the merging of red (raw fluorescence) and green (surface reconstruction) channels in the top panel, 3V: third ventricle, AW: anterior wall, CeC: central amygdala capsular division, CeL: central amygdala lateral division, CeM: central amygdala medial division, cst: commissural stria terminalis, LVID, d and LVID, s: left ventricle internal dimensions in diastole and systole, PVN: paraventricular nucleus, PW: posterior wall.

Figure S2

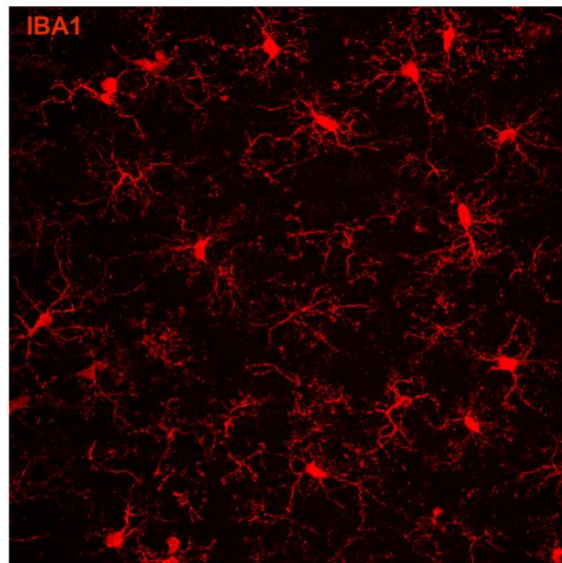


**Figure S2: Sham surgery per se does not alter the morphology of PVN or CeA microglia** (a) brain scheme shows the topographic location of PVN microglia that have been used for the morphometric assessment. The red area within the PVN (heart-shaped nucleus) highlights the fraction of the nucleus where pictures were taken, (b) dot-plot graphs show the individual values of PVN microglia for surface area, cell volume, filament length and IBA 1 intensity for the non-surgery control (N=357 cells from 4 rats), and sham rats at 8, 14 and 16 weeks post-surgery (N=381 cells from 4 rats, N= 365 cells from 4 rats and N=389 cells from 4 rats, respectively), one-way ANOVA was used to analyze the data followed by Tukey post-hoc test, (c) brain scheme shows the topographic location of CeA microglia that have been used for the morphometric assessment. The red area within the CeA highlights the divisions where pictures were taken, (d) dot-plot graphs show the individual values of CeA microglia for surface area, cell volume, filament length and IBA 1 intensity for the non-surgery control (N=297 cells from 4 rats), and sham rats at 8, 14 and 16 weeks post-surgery (N=377 cells from 4 rats, N=339 cells from 4 rats and N=354 cells from 4 rats, respectively).

(A) S1BF microglia sham 16w



S1BF microglia HF 16w **Figure S3**



(B)



(C)

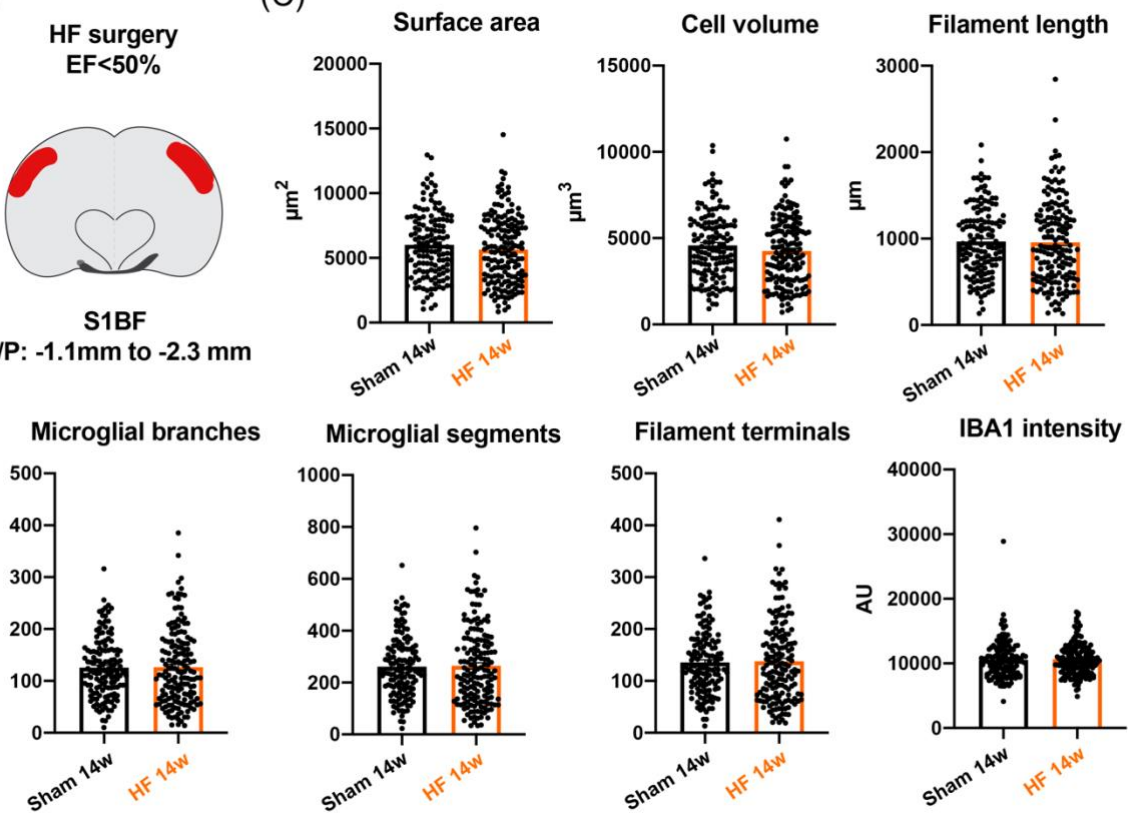


**Figure S3: HF does not induce morphometric changes in somatosensory cortex 1 barrel field microglia** (a) representative confocal images show IBA1-stained microglia in the S1BF of HF and sham rats 16 weeks post-surgery, (b) brain scheme shows the topographic location of S1BF microglia that have been used for the morphometric assessment. The red area highlights the S1BF, (c) dot-plot graphs show the individual values of S1BF microglia for surface area, cell volume, filament length, microglial branches, microglial segments, filament terminals and IBA 1 intensity for sham rats (n=4) and HF rats (n= 4). One-way ANOVA was used to analyze the data.



(A) Sham 16w HF surgery EF>50% 16w Figure S4

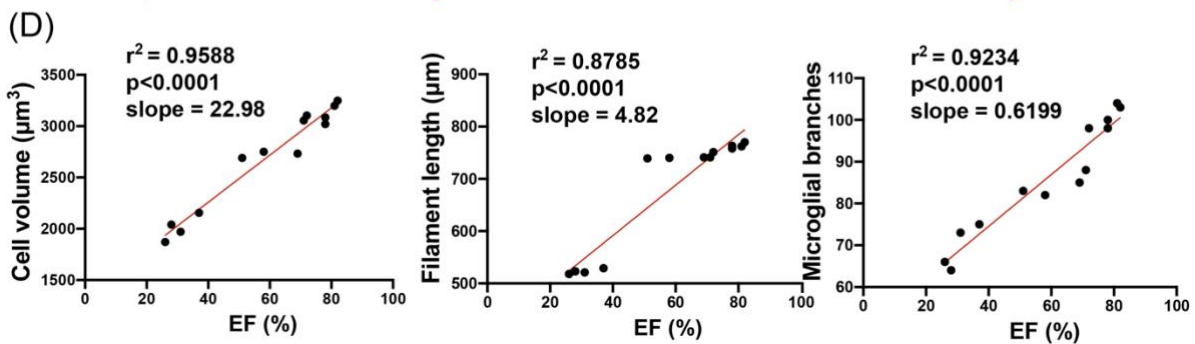
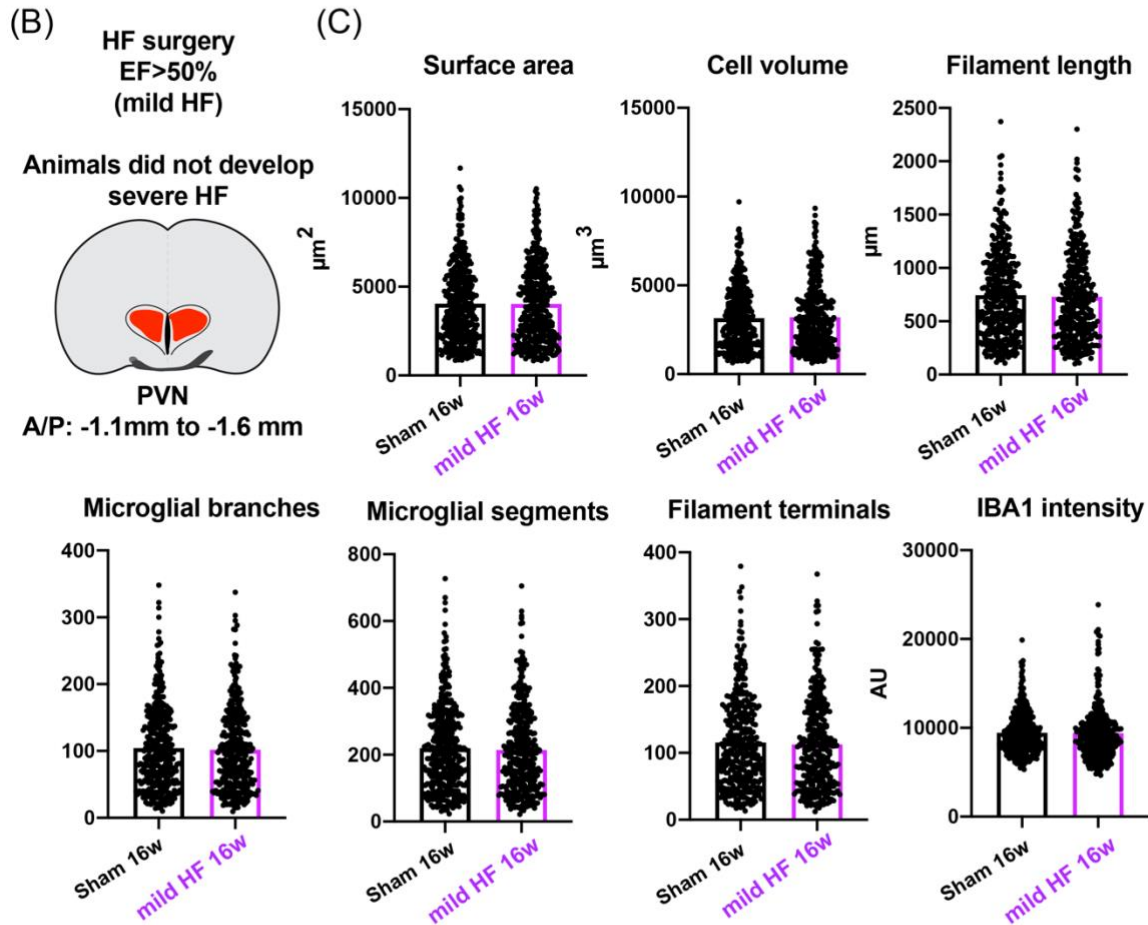
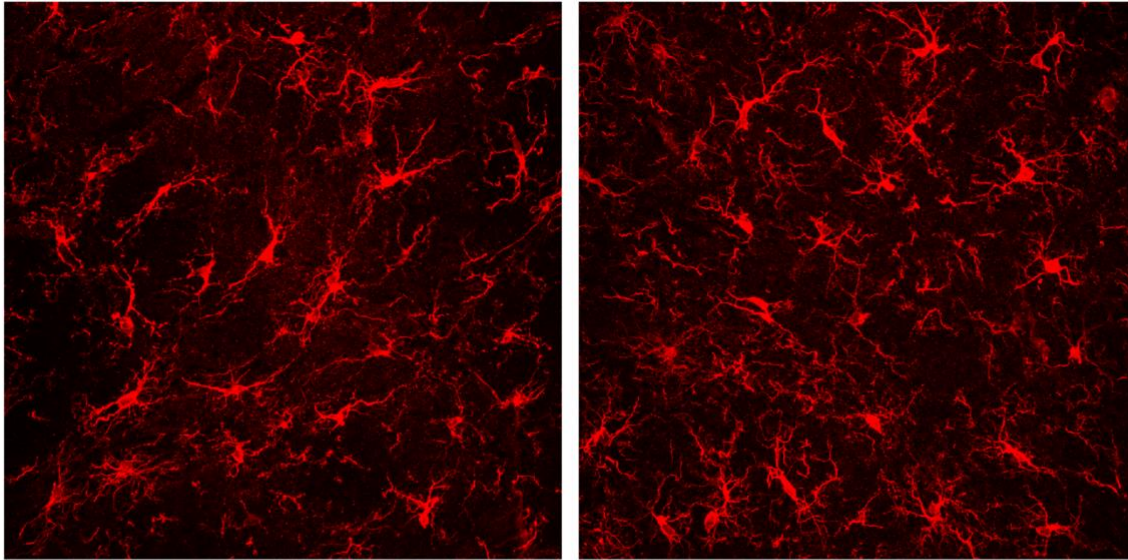


**Figure S4: Morphological changes in microglia are not observed in rats with mild level of HF** (a) representative confocal images show IBA1-stained microglia in the PVN of sham and rats that underwent heart failure surgery, but did not develop severe HF ('mild HF'), indicated by an ejection fraction greater than 50% (EF>50%), (b) brain scheme shows the topographic location of PVN microglia that have been used for the morphometric assessment. The red area highlights the PVN, (c) dot-plot graphs show the individual values of PVN microglia for surface area, cell volume, filament length, microglial branches, microglial segments, filament terminals and IBA 1 intensity for sham rats (n=4) and mild HF rats (n=5). One-way ANOVA was used to analyze the data, (d) plot graphs depicting cell volume, filament length and number of microglial branches as a function of %EF values combining sham (n=4), HF rats (EF<50%, n=4) and mild HF rats (EF>50%, n=5). R<sub>2</sub> and p values were obtained following a Pearson correlation analysis.



Figure S5

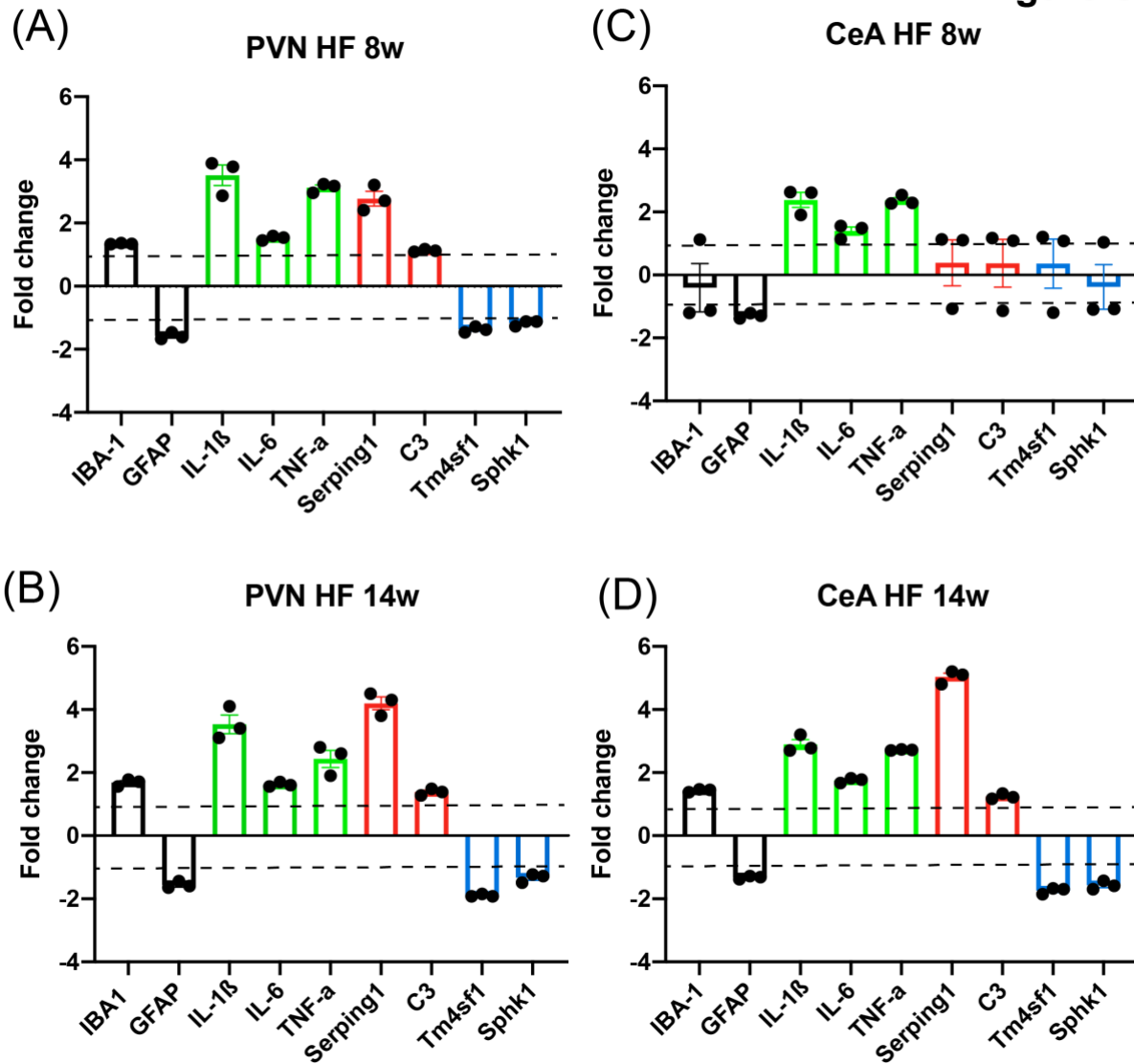


**Figure S5: HF-induced changes in neuroinflammation-associated microglia and astrocyte marker mRNA levels** (a-f) bar graphs show the mean fold change in mRNA transcript levels in HF rats compared to sham rats in the PVN (a, b) and the CeA (c, d). All graphs depict the fold changes of mRNA levels in HF group compared to their respective shams. Green bars: cytokines, red bars: a1 astrocyte markers, blue bars: a2 astrocyte markers. Dashed lines indicate the hypothetical mean (+1/-1) for the one-sample t-test. Each dot represents the average value of the pooled samples and the measurements were performed in triplicates. \* $p < 0.05$ , \*\* $p < 0.01$  and \*\*\* $p < 0.0001$  vs. respective controls, one sample t-test.